

# SPHERICAL COLLAPSE FOR A VISCOUS GENERALIZED CHAPLYGIN GAS MODEL

*Wei Li<sup>a,b\*</sup>, Lixin Xu<sup>a\*\*</sup>*

*<sup>a</sup>Institute of Theoretical Physics, School of Physics and Optoelectronic Technology,  
Dalian University of Technology  
116024, Dalian, China*

*<sup>b</sup>Department of Physics, Bohai University  
121013, Jinzhou, China*

Received September 2, 2014

The nonlinear collapse for a viscous generalized Chaplygin gas model (VGCG) is analyzed in the framework of spherical top-hat collapse. Because the VGCG and baryons are essential to form the large-scale structure, we focus on their nonlinear collapse in this paper. We discuss the influence of model parameters  $\alpha$  and  $\zeta_0$  on the spherical collapse by varying their values and compare with the  $\Lambda$ CDM model. The results show that for the VGCG model, smaller  $\zeta_0$  and larger  $\alpha$  make the structure formation earlier and faster, and the collapse curves of the VGCG model are almost coincident with those of the  $\Lambda$ CDM model when the model parameter  $\alpha$  is less than  $10^{-2}$ .

DOI: 10.7868/S0044451015040059

## 1. INTRODUCTION

In recent years, an increasing number of cosmological observations suggest that our universe is filled with an imperfect fluid that includes bulk viscosity in its negative pressure; this pressure was dubbed the effective pressure, as was argued in [1, 2]. Based on this condition, viscous generalized Chaplygin gas models [3–7] were extensively investigated as competitive models to be used in explaining the late-time accelerated expansion of the universe. In these papers, the viscous generalized Chaplygin gas (VGCG) model unified dark energy and cold dark matter into a unique imperfect dark fluid, which retains the property of simulating the  $\Lambda$ CDM model well on the background level.

Usually, the bulk viscosity is chosen to be a density-dependent or time-dependent function. A density-dependent viscosity coefficient  $\zeta = \zeta_0 \rho^m$  is widely investigated in the literature, with  $\zeta_0 > 0$  ensuring a positive entropy in agreement of the second law of thermodynamics. In our previous work [4, 5], we studied the case  $m = 1/2$ , and obtained good results in line

with the cosmic observations. If a model cannot describe the observed large-scale structure and the background evolution, it should be ruled out because of a conflict among the cosmic observations and the theoretical calculation, and the VGCG model is no exception. Because the universe's original perturbations are the seed of the large-scale structure, investigating the evolution of density perturbations of a realistic cosmological model becomes very important. During this process, the study of nonlinear perturbations is inevitable. To the best of our knowledge, hydrodynamical/ $N$ -body numerical simulation (see, e. g., [8–11]) is a cumbersome task, which is typically used in dealing with a fully nonlinear analysis. Fortunately, there is a simple framework to solve this issue. In [15], the nonlinear collapse of a general Chaplygin gas model [16] was investigated in the framework of spherical top-hat collapse. The authors concluded that with increasing the value of  $\alpha$ , the growth of the structure becomes faster. In this paper, we expand their work by considering bulk viscosity in the general Chaplygin gas model (VGCG). Besides the parameter  $\alpha$ , we also analyze the effect of the bulk viscosity  $\zeta_0$  on the structure formation in the VGCG model with a spherically symmetric perturbation.

The paper is organized as follows. In Sec. 2, we give a brief review of the VGCG model and present some

\*E-mail: liweizhd@126.com

\*\*E-mail: lxxu@dlut.edu.cn; corresponding author

basic equations for spherical top-hat collapse. Section 3 describes the method and main results. The conclusion is presented in the last section.

## 2. THE BASIC EQUATIONS FOR SPHERICAL TOP-HAT COLLAPSE IN THE VGCG MODEL

In an isotropic and homogeneous universe, the effective pressure of a VGCG model [4, 5] is given in the form [14–16]

$$p_{VGCG} = -\frac{A}{\rho_{VGCG}^\alpha} - \sqrt{3}\zeta_0\rho_{VGCG}, \quad (1)$$

and the equation of energy density is

$$\rho_{VGCG} = \rho_{GCG0} \left[ \frac{B_s}{1 - \sqrt{3}\zeta_0} + \left( 1 - \frac{B_s}{1 - \sqrt{3}\zeta_0} \right) \times a^{-3(1+\alpha)(1-\sqrt{3}\zeta_0)} \right]^{1/(1+\alpha)}, \quad (2)$$

where  $B_s = A/\rho_{GCG0}^{1+\alpha}$ ,  $\alpha$  and  $\zeta_0$  are model parameters, and we require that  $0 \leq B_s \leq 1$  and  $\zeta_0 < 1/\sqrt{3}$ . We can obtain the standard  $\Lambda$ CDM model when  $\alpha = 0$  and  $\zeta_0 = 0$ . By considering the VGCG as a unified component and taking the assumption of a purely adiabatic perturbations, it is easy to obtain the Friedmann equation

$$H^2 = H_0^2 \left\{ (1 - \Omega_b - \Omega_r - \Omega_k) \left[ \frac{B_s}{1 - \sqrt{3}\zeta_0} + \left( 1 - \frac{B_s}{1 - \sqrt{3}\zeta_0} \right) a^{-3(1+\alpha)(1-\sqrt{3}\zeta_0)} \right]^{1/(1+\alpha)} + \Omega_b a^{-3} + \Omega_r a^{-4} + \Omega_k a^{-2} \right\}, \quad (3)$$

and the effective adiabatic sound speed for the VGCG:

$$c_{ad,eff}^2 = \frac{\dot{p}_{VGCG}}{\dot{\rho}_{VGCG}} = -\alpha w_{eff} - \sqrt{3}\zeta_0, \quad (4)$$

where  $w_{eff}$  is the EoS of the VGCG in the form of

$$w_{eff} = w - \sqrt{3}\zeta_0 = -\frac{B_s}{B_s + (1 - B_s)a^{-3(1+\alpha)}} - \sqrt{3}\zeta_0. \quad (5)$$

Because of the negative values of  $w_{eff}$ ,  $\alpha \geq 0$  is required in order to ensure that the speed of sound is nonnegative.

The spherical collapse (SC), which provides a way to glimpse into the nonlinear regime of the perturbation theory, was introduced first by Gunn and Gutt

1972 [17]. Following the assumption of a top-hat profile (that the density perturbation is uniform throughout the collapse), the evolution of the perturbation is only time-dependent. In other words, we can omit the gradients inside the perturbed region, as was done in [12].

In the spherical top-hat collapse (SCTH) model, the equations for background evolution are

$$\dot{\rho} = -3H(\rho + p), \quad (6)$$

$$\frac{\ddot{a}}{a} = -\frac{4\pi G}{3} \sum_i (\rho_i + 3p_i), \quad (7)$$

and the basic equations in the perturbed region are

$$\dot{\rho}_c = -3h(\rho_c + p_c), \quad (8)$$

$$\frac{\ddot{r}}{r} = -\frac{4\pi G}{3} \sum_i (\rho_{ci} + 3p_{ci}), \quad (9)$$

where  $\rho_c = \rho + \delta\rho$  and  $p_c = p + \delta p$  are the perturbed quantities, and  $h$  is related to  $H$  in the STHC framework as

$$h = H + \frac{\theta}{3a}, \quad (10)$$

where  $\theta \equiv \nabla \cdot \mathbf{v}$  is the divergence of the peculiar velocity  $\mathbf{v}$ .

Hence, the equations for density contrast  $\delta_i = (\delta\rho/\rho)_i$  and  $\theta$  are [12, 18]

$$\dot{\delta}_i = -3H(c_{ei}^2 - w_i)\delta_i - [1 + w_i + (1 + c_{ei}^2)\delta_i] \frac{\theta}{a}, \quad (11)$$

$$\dot{\theta} = -H\theta - \frac{\theta^2}{3a} - 4\pi G a \sum_i \rho_i \delta_i (1 + 3c_{ei}^2), \quad (12)$$

where the effective speed of sound is  $c_{ei}^2 = (\delta p/\delta\rho)_i$ , where  $i$  stands for different energy components. Equations (11) and (12) can be rewritten in a form with the scale factor  $a$ ,

$$\delta'_i = -\frac{3}{a}(c_{ei}^2 - w_i)\delta_i - [1 + w_i + (1 + c_{ei}^2)\delta_i] \frac{\theta}{a^2 H}, \quad (13)$$

$$\theta' = -\frac{\theta}{a} - \frac{\theta^2}{3a^2 H} - \frac{3H}{2} \sum_i \Omega_i \delta_i (1 + 3c_{ei}^2), \quad (14)$$

where we use the definition  $\Omega_i = 8\pi G\rho_i/3H^2$ .

From the above equations, we can find that  $w_c$  and  $c_e^2$  are important quantities. The definition of the equation of state  $w_c$  is

$$w_c = \frac{p + \delta p}{\rho + \delta\rho} = \frac{w_{eff}}{1 + \delta} + c_e^2 \frac{\delta}{1 + \delta}, \quad (15)$$

and the most important effective speed of sound is

$$c_e^2 = \frac{\delta p}{\delta\rho} = \frac{p_c - p}{\rho_c - \rho} = -\alpha w_{eff} - \sqrt{3}\zeta_0. \quad (16)$$

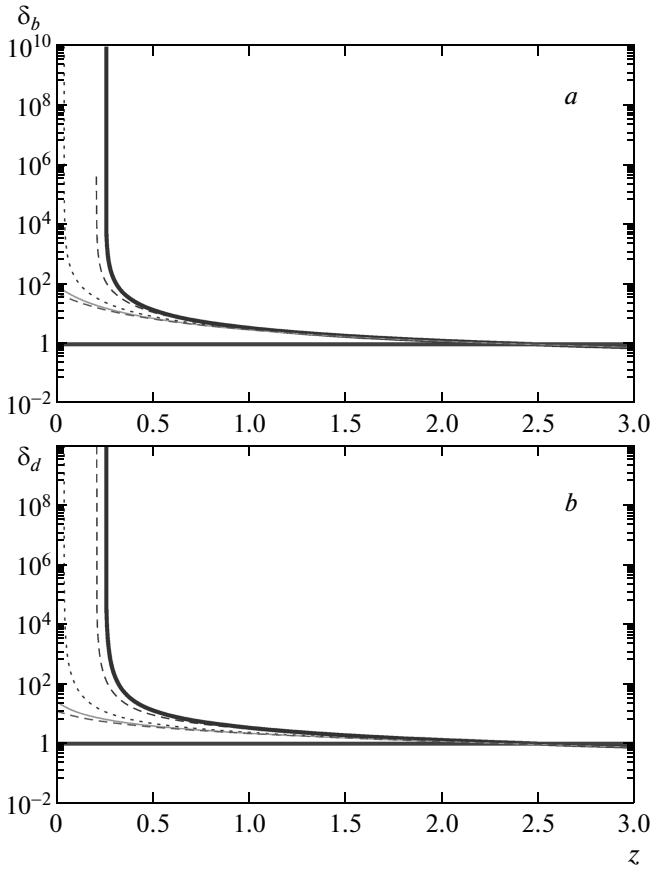


**Fig. 1.** The evolutions of density perturbations with respect to the redshift for VGCG models, where the bulk viscosity coefficient is fixed at  $\zeta_0 = 0.000708$ . The thick, dashed, dotted, thin grey solid, and grey dashed lines are for  $\alpha = 1, 0.5, 0.1, 0.01, 0$  respectively, for baryons (a) and the VGCG (b). The horizontal line  $\delta = 1$  denotes the limit of linear perturbation and the vertical parts of curved lines are the collapse of the perturbed regions

### 3. THE METHOD AND RESULTS

To study the nonlinear evolution of the baryon and VGCG perturbations in the framework of spherical top-hat collapse, we perform a mathematical simulation via the software Mathematica. In this process, we solve differential equations (13) and (14) with the initial conditions  $\delta_d(z = 1000) = 3.5 \cdot 10^{-3}$ ,  $\delta_b(z = 1000) = 10^{-5}$ , and  $\theta = 0$ , which are the conditions used in Ref. [12, 19].

To show the influence of the model parameter  $\alpha$  and  $\zeta_0$  on the spherical collapse, we let the other relevant cosmological model parameters take their central values  $H_0 = 70.324 \text{ km} \cdot \text{s}^{-1} \cdot \text{Mpc}^{-1}$ ,  $\Omega_d = 0.954$ ,  $\Omega_b = 0.046$ , and  $B_s = 0.766$ , which were obtained in Ref. [4]. We first investigate the impact of the parameter  $\alpha$  on the

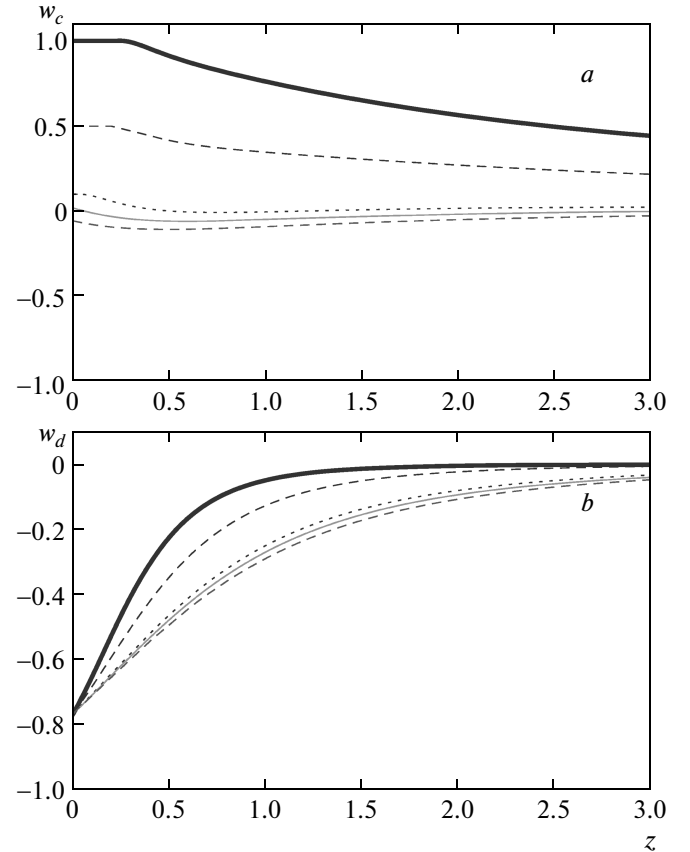


**Fig. 2.** The evolutions of  $w_c$  and  $w_d$  with respect to the redshift  $z$  for VGCG models, where the thick, dashed, dotted, grey solid and grey dashed curved lines are for  $\alpha = 1, 0.5, 0.1, 0.01, 0$  respectively for  $w_c$  (a) and  $w_d$  (b)

**Table.** Models for the STHC model, where the values of  $\alpha$  are small nonnegative values because of the constraint from background evolution. Note that model “a” is identical to the  $\Lambda$ CDM model. The redshift  $z_{ta}$  is the turnaround redshift when the collapse of the perturbed region begins

Model	$\alpha$	$\zeta_0$	$B_s$	$z_{ta}$
a	0	0	0.766	0.104
b	0.01	0.000708	0.766	0.128
c	0.1	0.000708	0.766	0.251
d	0.5	0.000708	0.766	0.667
e	1	0.000708	0.766	0.785

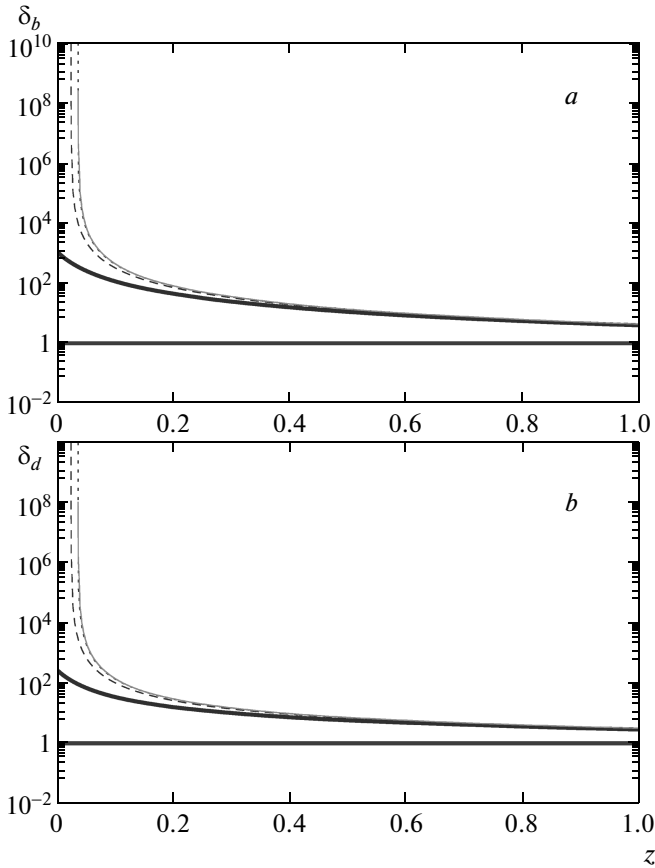


**Fig. 3.** The evolutions of density perturbations with respect to the redshift for VGCG models, where the model parameter is fixed at  $\alpha = 0.035$  and the thick, dashed, dotted and grey solid curved lines are for  $\zeta_0 = 10^{-3}, 10^{-4}, 10^{-5}, 0$  respectively for baryons (a) and the VGCG (b). The horizon line  $\delta = 1$  denotes the limit of linear perturbation and the vertical parts of the curved lines are the collapse of the perturbed regions

nonlinear collapse. By fixing  $\zeta_0 = 0.000708$ , which is obtained in our previous work [4] and varying the model parameter  $\alpha = 1, 0.5, 0.1$ , and  $0.01$ , we obtain the results shown in Table and in Figs. 1 and 2, where  $z_{ta}$  is the turnaround redshift when the collapse of the perturbed region begins. We also plot the collapse curves of the  $\Lambda$ CDM model using the grey dashed curves in the two figures above to compare it with the VGCG model. From these results, we can conclude that the perturbations collapse earlier for the larger values of  $\alpha$ ; furthermore, the collapse curves of the VGCG model are almost coincident with those of the  $\Lambda$ CDM model when the model parameter  $\alpha$  is less than  $10^{-2}$ . This conclusion is the same as the result obtained in the previous papers, such as Ref. [12, 19].

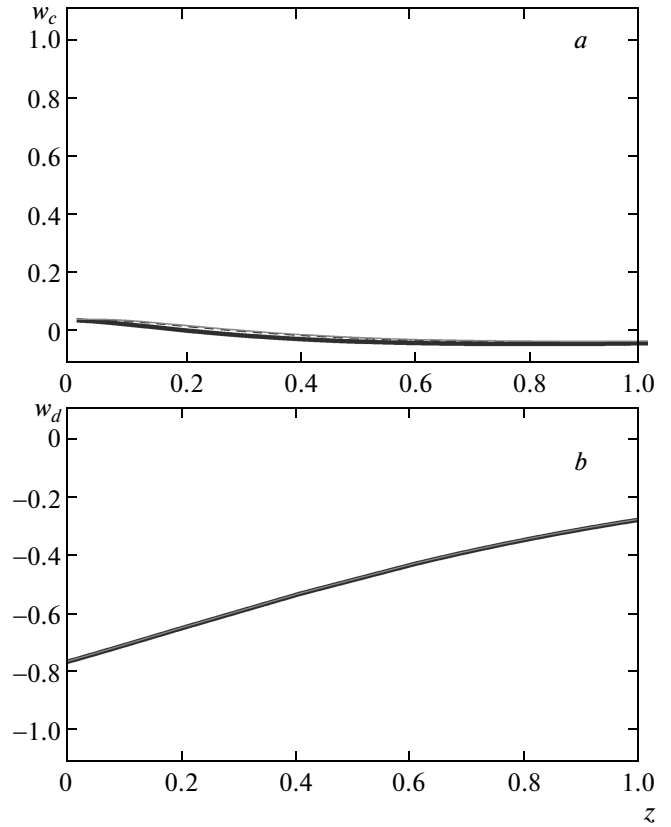


**Fig. 4.** The evolutions of  $w_c$  and  $w_d$  with respect to the redshift  $z$  for the VGCG model with  $\alpha = 0.035$ , where the thick, dashed, dotted, and grey solid curved lines are for  $\zeta_0 = 10^{-3}, 10^{-4}, 10^{-5}, 0$  respectively for  $w_c$  (a) and  $w_d$  (b)

Next, we show the effect of  $\zeta_0$  on the evolution of density perturbations in the VGCG model. Here, we fix  $\alpha = 0.035$ , which is borrowed from our previous work [4], and change the bulk viscosity values to  $\zeta_0 = 0.001, 0.0001, 0.00001$ , and  $0$ . The corresponding evolutions of density perturbations of baryon matter and the VGCG are shown in Fig. 3 and the evolution of the EoS parameter is displayed in Fig. 4. In Fig. 3, the horizontal line  $\delta = 1$  denotes the linear perturbation limit and the vertical parts of the curved lines stands for the perturbed region collapse, whence we can conclude that the smaller bulk viscosity coefficient  $\zeta_0$  can lead to the earlier collapse, that is to say, the larger the value of  $\zeta_0$  is, the later the collapse occurs. Therefore, this is the reason why the bulk viscosity coefficient  $\zeta_0$  should not be too large.

From the analysis above, we can clearly understand the impact of the model parameters  $\zeta_0$  and  $\alpha$  on the evolution of density perturbations. In addition, we can

conclude that the influence of  $\alpha$  is conspicuous as expected, because  $\alpha$  is strongly linked with the effective speed of sound of the perturbations.

#### 4. CONCLUSION

We have discussed the structure formation of the viscous generalized Chaplygin gas model in the spherical top-hat collapse framework. We studied the effects of  $\zeta_0$  and  $\alpha$  on the nonlinear perturbation evolution via choosing their different values and compare with the  $\Lambda$ CDM model. On the basis of the calculations and analysis, we can conclude that large  $\alpha$  and small  $\zeta_0$  can lead to an earlier and faster collapse, and when the model parameter  $\alpha$  is less than  $10^{-2}$ , the collapse curves of the VGCG model almost overlap with those of the  $\Lambda$ CDM model. In the next work, we will try to study nonlinear collapse by using the hydrodynamic/ $N$ -body numerical simulation.

L. Xu's work is supported in part by NSFC under the Grant No. 11275035 and the Fundamental Research Funds for the Central Universities under the Grant No. DUT13LK01.

#### REFERENCES

1. A. B. Balakin, D. Pavon, D. J. Schwarz, and W. Zimdahl, *New J. Phys.* **5**, 85 (2003).
2. W. Zimdahl, D. J. Schwarz, A. B. Balakin, and D. Pavon, *Phys. Rev. D* **64**, 063501 (2001).
3. C. S. J. Pun, L. Gergely, M. K. Mak, Z. Kovcs, G. M. Szab, and T. Harko, *Phys. Rev. D* **77**, 063528 (2008); arXiv:0801.2008v1 [gr-qc].
4. Wei Li and Lixin Xu, *Eur. Phys. J. C* **73**, 2471 (2013), DOI:10.1140/epjc/s10052-013-2471-1.
5. Wei Li and Lixin Xu, *Eur. Phys. J. C* **74**, 2765 (2014), DOI:10.1140/epjc/s10052-014-2765-y.
6. Xiang-Hua Zhai, You-Dong Xu, and Xin-Zhou Li, *Int. J. Mod. Phys. D* **15**, 1151 (2006); arXiv:astro-ph/0511814.
7. A. R. Amani and B. Pourhassan, *Int. J. Theor. Phys.* **52**, 1309 (2013), DOI:10.1007/s10773-012-1446-6.
8. A. V. Maccio', C. Quercellini, R. Mainini, L. Amendola, and S. A. Bonometto, *Phys. Rev. D* **69**, 123516 (2004).
9. N. Aghanim, A. C. da Silva, and N. J. Nunes, *Astron. Astrophys.* **496**, 637 (2009).
10. M. Baldi, V. Pettorino, G. Robbers, and V. Springel, *Mon. Not. Roy. Astron. Soc.* **403**, 1684 (2010).
11. B. Li, D. F. Mota, and J. D. Barrow, *Astrophys. J.* **728**, 109 (2011).
12. R. A. A. Fernandes, J. P. M. de Carvalho, A. Yu. Kamenshchik, U. Moschella, and A. da Silva, *Phys. Rev. D* **85**, 083501 (2012).
13. Kazuharu Bamba, Salvatore Capozziello, Shin'ichi Nojiri, S. D. Odintsov, *Astrophys. Space Sci.* **342**, 155 (2012), DOI:10.1007/s10509-012-1181-8; arXiv:1205.3421 [gr-qc].
14. S. Capozziello, V. F. Cardone, E. Elizalde, S. Nojiri, and S. D. Odintsov, *Phys. Rev. D* **73**, 043512 (2006), DOI:10.1103/PhysRevD.73.043512; arXiv:astro-ph/0508350.
15. Shin'ichi Nojiri and S. D. Odintsov, *Phys. Rev. D* **72**, 023003 (2005), DOI:10.1103/PhysRevD.72.023003; arXiv:hep-th/0505215.
16. I. Brevik and S. D. Odintsov, *Phys. Rev. D* **65**, 067302 (2002), DOI:10.1103/PhysRevD.65.067302; arXiv:gr-qc/0110105.
17. J. E. Gunn and J. R. Gott, *Astrophys. J.* **176**, 1 (1972).
18. L. R. Abramo, R. C. Batista, L. Liberato, and R. Rosenfeld, *Phys. Rev. D* **79**, 023516 (2009).
19. Lixin Xu, *Eur. Phys. J. C* **73**, 2344 (2013), DOI:10.1140/epjc/s10052-013-2344-7; arXiv:1302.6637 [astro-ph.CO].